PHYSICAL REVIEW B VOLUME 18, NUMBER 1 1 JULY 1978

Resistivity of amorphous ferromagnetic Fe_cAu_{1-c} alloys: Anisotropy and field dependence

G. Bergmann and P. Marquardt
Institut für Festkörperforschung der KFA Jülich, Postfach 517, Jülich, Federal Republic of Germany
(Received 3 November 1977)

Owing to their spontaneous magnetization, amorphous ferromagnetic metals exhibit a direction of preference. Hence, the electrical resistivity is anisotropic and consists of three main components: the longitudinal resistivity $\rho_\parallel$, the transverse resistivity $\rho_\perp$, and the spontaneous Hall resistivity $\rho_H(0)$. These contributions also show a distinct dependence on the applied magnetic field. In this article, we present our experimental studies of the amorphous ferromagnetic alloy system Fe_cAu_{1-c} ($0.45 \leq c \leq 0.97$). Most of the measured variables show a pronounced concentration dependence above $c = 0.9$. This is correlated with the sudden drop of the magnetic moment of the Fe atoms above $c = 0.9$. The high-field Hall effect in principle allows a determination of the effective number of conduction electrons. In the discussion we generalize the single-site approximation for the resistivity of amorphous and liquid transition metals to amorphous ferromagnets. In the framework of the phase-shift treatment of the resistivity, the spin-up and spin-down conduction electrons are scattered according to different phase shifts $\rho_2^\uparrow$ and $\rho_2^\downarrow$. Numerical calculations of the resistivity are performed and demonstrate the strong sensitivity of the calculated ρ on the various parameters. The anisotropy effects are semiquantitatively discussed by extension of a model due to Fert and Jaoul.

I. INTRODUCTION

In recent years, the properties of ferromagnetic metallic glasses and amorphous metals have evoked an increasing interest in scientific and technical investigations. For the sake of clarity, we distinguish the two systems carefully in this article. Noncrystalline metallic alloys which are stabilized by adding about 20 at.% of so-called glass formers (C, P, Ge, Si, B, etc.) shall be qualified as *metallic glasses*. Purely metallic alloys with a noncrystalline structure will be called *amorphous metals*. Metallic glasses are generally produced by splat cooling. Their crystallization temperatures often reach far beyond room temperature. Amorphous metals are usually obtained by quenched condensation onto a substrate at very low temperature. Their crystallization temperatures vary from 40 K (pure amorphous Co) up to several hundred °C (e.g., $Ni_{0.65}Au_{0.35}$).[1] Although the magnetic properties of these amorphous systems have been dealt with in several surveys,[2-7] their electronic structure still remains quite unknown.

In the metallic glasses, the glass formers give rise to high thermal stability. This practical advantage, however, has been traded for the disadvantage of more complicated physical and electronic properties. The electronic binding between the metal atoms and the polyvalent glass-former atoms is more difficult to describe. Above all, it is not clear how the valence electrons of the glass formers participate in the conduction mechanism. Therefore amorphous metals and alloys are much better suited for the investigation of the electronic structure. An understanding of their properties should be sought first. Then we can hope that an extension to metallic glasses will be more promising. We have investigated the electronic transport properties of amorphous ferromagnetic alloys of the composition T_cAu_{1-c} (where T is a transition metal, Fe, Co, or Ni) in a series of former papers.[8-12]

The magnetization of amorphous ferromagnetic alloys induces a direction of preference. In these structurally isotropic systems the anisotropic effects due to the magnetization are not obscured by any other direction-dependent properties. Hence it is most instructive to consider the transport phenomena in an amorphous ferromagnet. Here, the resistivity depends on the relative orientation between the magnetization $\vec{J}$ and the current $\vec{j}$. The anisotropy is most suitably represented by a tensor which contains three independent parts: the longitudinal resistivity $\rho_\parallel$ ($\vec{j} \parallel \vec{J}$), the transverse resistivity $\rho_\perp$ ($\vec{j} \perp \vec{J}$), and the spontaneous Hall resistivity $\rho_H(0)$. Additionally, an applied magnetic field B will give rise to magnetoresistance effects that are much larger than predicted by the Kohler rule.[13]

The experimental section of this article focuses on the various components of the resistivity in the amorphous Fe_cAu_{1-c} system ($0.45 \leq c \leq 0.97$). Resistivity measurements are presented as a function of the applied field B and of the Fe concentration c. Above 90-at.% Fe, the magnetic moment per Fe atom decreases abruptly.[14] This feature clearly manifests itself in the concentration-dependent transport phenomena. The resistivity $\rho(c)$ exhibits a kink. In addition, $\rho(T)$ has a dis-

tinct minimum for $c > 0.9$. The magnetoresistance $|\partial\rho/\partial B|$ shows a pronounced maximum and the anomalous Hall effect shows a dramatic increase with c.

The Fe_cAu_{1-c} system has also been studied extensively in the liquid state.[15,16] Since the structure factors in the amorphous and in the liquid states are quite similar, a comparison between the two states is straightforward. In the amorphous state, the magnetic moments are aligned ferromagnetically whereas they are randomly oriented in the liquid paramagnetic state. These different spin orientations lead to distinctly different transport properties.

In the theoretical section, we shall try to extend the models developed so far for the resistivity of amorphous alloys[17-20] to magnetic systems. The anisotropy effects are interpreted as originating in the spin-orbit splitting of the d states which Fert and Jaoul[21] introduced for isolated atoms. We shall critically discuss the theoretical results and perform a quantitative comparison with the experimental resistivities.

II. EXPERIMENTAL PROCEDURE, NOMENCLATURE, AND RESULTS

The amorphous Fe_cAu_{1-c} films ($0.45 \leq c \leq 0.97$) are obtained by quenched condensation of the alloy onto a quartz substrate kept at liquid-He temperature. Felsch[14] demonstrated by x-ray structure investigations that quench condensed Fe_cAu_{1-c} films are amorphous within the concentration range mentioned above. During annealing, the films undergo an irreversible transformation into the crystalline state at some crystallization temperature depending on their composition. Such a phase transition is always accompanied by a more or less sudden drop in the resistance which we regard as criterion for amorphicity in our experiments [see, for example, the annealing effect on $\rho(T)$ of a $Fe_{0.90}Au_{0.10}$ film in Fig. 1].

Over quite a large temperature range, Au and Fe have pratically the same vapor pressure.[22] Therefore the concentration in the condensed film is not changed by the evaporation process. This we demonstrated by using a single alloy several times without finding a severe shift of the crystallization temperature. An independent concentration check by means of x-ray fluorescence spectroscopy yielded values within 5 at.% of the original concentrations. Besides forcing the Fe into the amorphous state and stabilizing it, the Au furthermore serves as a gradual "dilution component" for the ferromagnetism of the films. The film thicknesses were measured with the aid of the Tolansky[23] multiple-beam interference technique. Thicknesses between 1000 and 1500 Å were used.

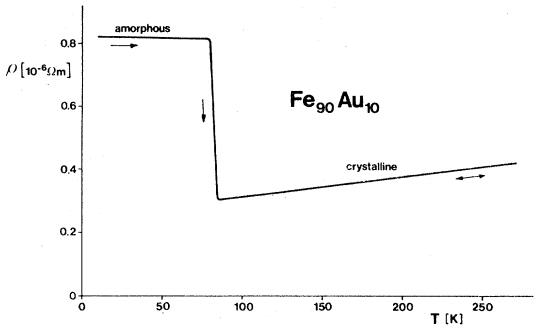

FIG. 1. Resistivity of a $Fe_{0.90}Au_{0.10}$ film during annealing. At about 80 K the film transforms from the amorphous into the crystalline state.

The essential details of the apparatus involved in the experiments have already been described in a previous paper.[24] For the determination of the resistance anisotropy the substrate holder in the evaporation cryostat has been modified as is seen in Fig. 2.

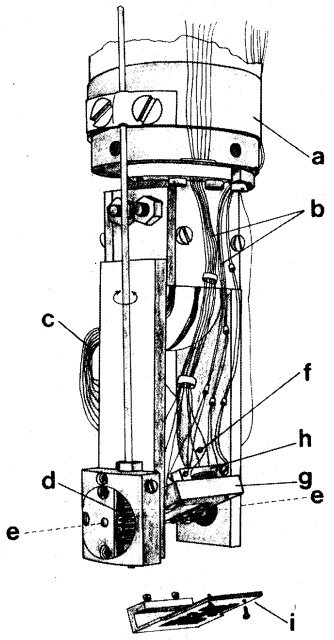

FIG. 2. Bottom part of our evaporation cryostat consisting of He tank (a) and rotatable sample holder (g) which is suspended by copper bars. The rotation about the axis e-e is performed by means of a worm and spur (d). Thermal coupling to (a) is achieved by flexible silver strips (c). The closing of an electrical circuit at (f) indicates the longitudinal orientation. The quartz substrate is mounted from below by means of the mask holder (i). Several thermometers are housed in part (h). The electrical leads are denoted by (b).

The substrate can be rotated about the axis $e-e$ in Fig. 2 by 90° with respect to the fixed direction of the applied magnetic field which we choose to be the z axis: $\vec{B}=(0,0,B)$. This enables us to investigate the transport properties of our Fe films with current $\vec{j}\perp\vec{B}$ as well as with $\vec{j}\parallel\vec{B}$. The thermal coupling to the He container (a) is maintained by flexible silver strips (c).

The current $\vec{j}$ is stabilized to 1 in 10^5 and the resistivities are evaluated using a $5\frac{1}{2}$ digit voltmeter. Our films are prepared with the shape shown in Fig. 3. The current flows from electrode 1 to 6. Starting with the transverse film orientation ($\vec{j}\perp\vec{B}$) after the condensation we determine the transverse resistivity $\rho_\perp(B)$ between electrodes 2 and 4 and the Hall resistivity $\rho_H(B)$ between electrodes 3 and 4. The field is varied between -6 and $+6$ V sec/m^2 (1 V sec/m$^2=10^4$ G). The longitudinal orientation ($\vec{j}\parallel\vec{B}$) is indicated by the closing of an electrical circuit at the contact (f) shown in Fig. 2.[25] With the current $\vec{j}$ adjusted parallel to $\vec{B}$ we determine $\rho_\parallel$ correspondingly between electrodes 2 and 4.

In order to keep track of all the various contributions to the transport properties we take a tensor representation $\underline{\rho}$ of the resistivity and put

$$\underline{\rho}=\rho_{is}\underline{1}+\underline{\rho}_s(J)+\underline{\rho}_\infty(B)\,. \tag{2.1}$$

The factor ρ_{is} of the unit tensor $\underline{1}$ is the normal isotropic part of the resistivity.

The term

$$\underline{\rho}_s(J)=\begin{bmatrix}-\frac{1}{3}(\rho_\parallel-\rho_\perp) & \rho_H(0) & 0\\ -\rho_H(0) & -\frac{1}{3}(\rho_\parallel-\rho_\perp) & 0\\ 0 & 0 & \frac{2}{3}(\rho_\parallel-\rho_\perp)\end{bmatrix}, \tag{2.2}$$

describes the anisotropy effects caused by the magnetization $\vec{J}$ of the films. There is a non-vanishing difference $\rho_\parallel-\rho_\perp$ between longitudinal and transverse resistivity and a "spontaneous" contribution $\rho_H(0)$ to the Hall resistivity which we obtain by extrapolating $\rho_H(B)$ to zero field.

The tensor

$$\underline{\rho}_\infty(B)=\begin{bmatrix}\frac{\partial\rho}{\partial B} & R_\infty & 0\\ -R_\infty & \frac{\partial\rho}{\partial B} & 0\\ 0 & 0 & \frac{\partial\rho}{\partial B}\end{bmatrix}B \tag{2.3}$$

contains the field dependence of ρ in the high-field region (note the index "∞"), namely, the magnetoresistance $\partial\rho/\partial B$ and the high-field Hall effect $R_\infty B$. According to our experimental results (see Fig. 5) there is no need to distinguish $\partial\rho_\parallel/\partial B$ and $\partial\rho_\perp/\partial B$, so we simply put $\partial\rho/\partial B$.

The total Hall resistivity can be written[26]

$$\rho_H=R_0B+R_sJ_z\,, \tag{2.4}$$

and clearly consists of two parts. R_0B is the normal Hall resistivity due to the Lorentz force. The anomalous Hall effect R_sJ_z is characteristic of a ferromagnet and in the low-field region it is the dominating effect. The measured high-field Hall constant R_∞ essentially consists of the normal Hall constant R_0. With the notation R_∞ we want to take into account a possible high-field dependence of R_s and a high-field susceptibility which cannot be excluded *a priori*.

In the following figures we shall present the characteristic effects with the aid of some examples. We start with the Hall resistivity $\rho_H(B)$ of the $Fe_{0.50}Au_{0.50}$ alloy (Fig. 4). According to the definition $U_H=\frac{1}{2}[U_H(B)-U_H(-B)]$ of the Hall voltage we find the dependence of ρ_H on B as presented. In the low-field range, $\rho_H(B)$ increases

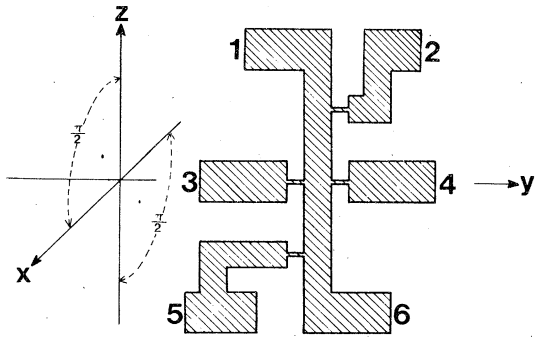

FIG. 3. Film geometry shown in the longitudinal orientation. The film can be rotated by 90° about the y axis into the transverse orientation.

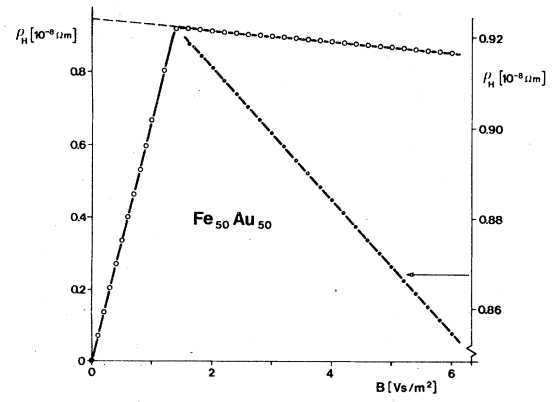

FIG. 4. Hall resistivty ρ_H as a function of applied field B for the $Fe_{0.50}Au_{0.50}$ alloy. The high-field part of ρ_H is separately drawn (full circles) on an enlarged scale.

proportional to B. Owing to the high-demagnetization factor of the film in the transverse orientation a large applied field B_s is required to twist the magnetization J perpendicular to the film plane. B_s is the saturation field, and, in absence of anisotropy fields, is identical to the saturation magnetization J_s.[27] As long as $B \leq B_s$ we have $B = J_z$ and observe a linear growth of ρ_H with B and consequently with J_z. The low field behavior of ρ_H thus constitutes the anomalous Hall effect $R_s J_z$, which saturates at B_s when the film is magnetized in z direction as is indicated by the kink of the curve. The high-field slope of ρ_H corresponds to a negative Hall constant R_∞. Its absolute value $|R_\infty|$ is smaller than R_s by almost two orders of magnitude. We plotted the high-field part of ρ_H separately against the enlarged scale on the right-hand side in Fig. 4 in order to demonstrate its linearity with B more clearly. Extrapolating the high-field part to zero field (see the dashed line) yields the spontaneous Hall resistivity $\rho_H(0)$.

Figure 5 shows $\rho_\parallel$ and $\rho_\perp$ of a $Fe_{0.65}Au_{0.35}$ film as a function of B. $B=0$ is a line of symmetry. The zero point of both $\rho_\parallel$ and $\rho_\perp$ has been strongly suppressed. Judging by the scale on the ordinate, the anisotropy $\rho_\parallel - \rho_\perp$ is of the order of 1% of the total resistivity.

In the longitudinal geometry, all demagnetization effects in the film are practically negligible. The magnetization is saturated by a very small applied field. Therefore a further increase of B affects only the high-field behavior of $\rho_\parallel$ and yields a linear decrease of $\rho_\parallel$ which we identify as the longitudinal magnetoresistance $\partial\rho_\parallel/\partial B$. In the transverse geometry, we meet the same situation with a maximal demagnetizating factor as in the case of ρ_H. In order to saturate J_z, a high-

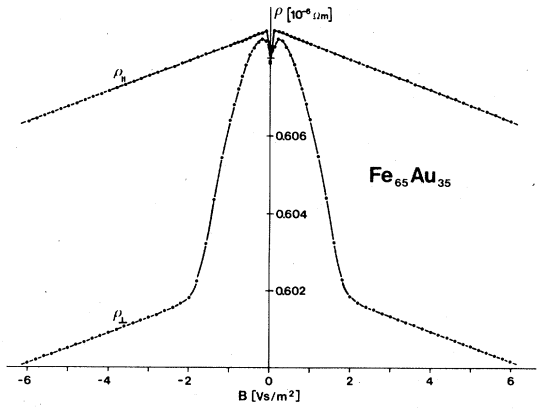

FIG. 5. Transverse and longitudinal resistivities $\rho_\perp$ and $\rho_\parallel$ of a $Fe_{0.65}Au_{0.35}$ film as a function of the applied field B.

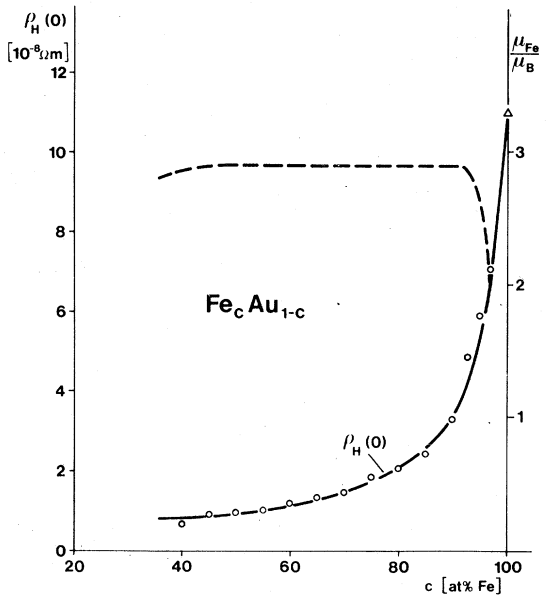

FIG. 6. Spontaneous Hall resistivity $\rho_H(0)$ of amorphous Fe_cAu_{1-c} alloys as a function of c (full curve). The dashed curve gives the magnetic moments of the Fe atoms in units of μ_B (right-hand scale) after Felsch (Ref. 14).

field B_s has to be applied. The transversal resistivity $\rho_\perp$ is determined at the kink of the curve, where the bell-shaped part levels off into the high-field behavior of $\rho_\perp$. For $B > B_s$, we find that the transversal magnetoresistance $\partial\rho_\perp/\partial B$ does not differ from $\partial\rho_\parallel/\partial B$ within our experimental accuracy. So we simply put $\partial\rho_\perp/\partial B = \partial\rho_\parallel/\partial B = \partial\rho/\partial B$ for both effects. In all our alloys $\partial\rho/\partial B < 0$. We define $\rho_\parallel(0) - \rho_\perp(B_s)$ as the resistance anisotropy. It describes the different scattering an electron wave experiences by a magnetic moment oriented parallel or perpendicular to the wave vector $\vec{k}$. Both $\rho_H(0)$ and $\rho_\parallel - \rho_\perp$ together reflect the total anisotropy of the transport properties which has its origin in the magnetization $\vec{J}$.

The vast concentration range ($0.45 \leq c \leq 0.97$) of amorphous Fe_cAu_{1-c} films is convenient for investigating the quantities mentioned so far as a function of c. Regarding first the Hall-effect results, we note a remarkable nonlinear increase of $\rho_H(0)$ towards the Fe-rich side of the Fe_cAu_{1-c} system (see Fig. 6). In a previous experiment, Koepke and Bergmann[28] succeeded in forcing an extremely thin pure-Fe film into the amorphous state. The $\rho_H(0)$ curve in Fig. 6 extrapolates to the value found for the pure amorphous film by the authors.

The characteristics we extract from the resistivity measurements (cf. Fig. 5) as a function of c are the negative magnetoresistance $\partial\rho/\partial B$ and

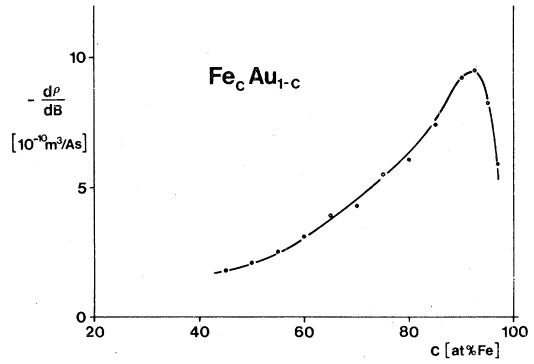

FIG. 7. Negative magnetoresistance $\partial\rho/\partial B$ of amorphous Fe_cAu_{1-c} alloys as a function of Fe concentration.

the anisotropy $\rho_\parallel - \rho_\perp$. Taking the absolute value of $\partial\rho/\partial B$ as a function of c we discover a pronounced maximum at $c \sim 92$ at.% Fe (see Fig. 7). Near the pure-Fe end of the abscissa, $\partial\rho/\partial B$ apparently drops to zero, a behavior observed likewise in amorphous Ni_cAu_{1-c} and Co_cAu_{1-c} films.[10,29]

The anisotropy $\rho_\parallel - \rho_\perp$ is found to be practically independent of c, as is demonstrated in Fig. 8. The experimental data correspond to a mean value of $\rho_\parallel - \rho_\perp \sim 0.7\times10^{-8}$ Ω m.

From Figs. 6 and 7 we conclude that the Fe_cAu_{1-c} system exhibits a special behavior at about 90-at.% Fe concentration. Another experimental clue to this emerges from the isotropic resistivity $\rho(c)$ shown in Fig. 9. For small Fe concentrations, ρ increases linearly with c and distinctly changes slope at $c \sim 0.9$.

We also measured the thermal effects on the resistivity and concentrated on the isotropic part $\rho(T)$ and the spontaneous Hall resistivity $\rho_H(T)$. The temperature dependence of $\rho(T)$ shows a remarkable behavior, too, at about 90% Fe. Due to

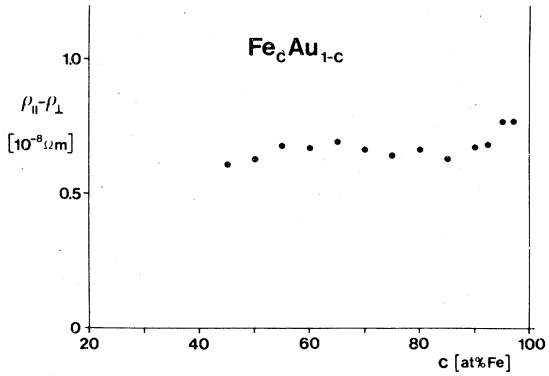

FIG. 8. Resistance anisotropy $\rho_\parallel - \rho_\perp$ of amorphous Fe_cAu_{1-c} alloys as a function of Fe concentration.

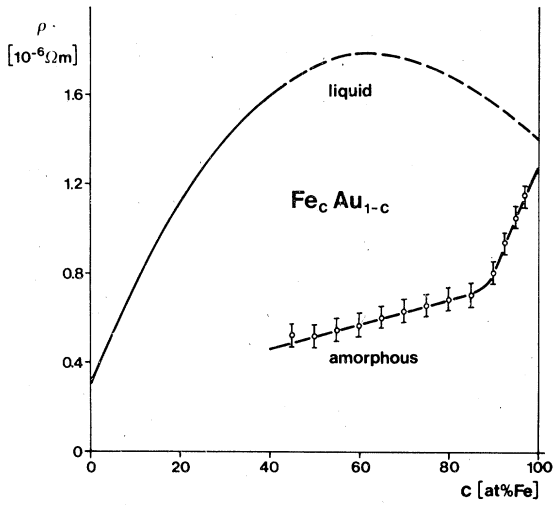

FIG. 9. Resistivity ρ of the amorphous Fe_cAu_{1-c} alloy series as a function of the concentration (lower curve; the uncertainties shown are limited by the thickness measuring technique). The upper curve represents the resistivities of the corresponding liquid alloys after Güntherodt and Künzi (Ref. 16).

scattering of electrons by thermally excited magnons, ρ generally obeys a T^2 law. Interestingly, we discover a resistivity minimum for $c \geq 0.9$. These results are represented elsewhere.[12] The temperature dependence of $\rho_H(0)$ is most conveniently studied in $Fe_{0.50}Au_{0.50}$ because it proves to be one of the most stable alloys (T_{cr} ~ 300 K). In Fig. 10 we choose T as parameter and plot $\rho_H(0)$ against ρ. This plot not only shows the linear growth of $\rho_H(0)$ with ρ, but also the increase with T. Since J_z diminishes the latter be-

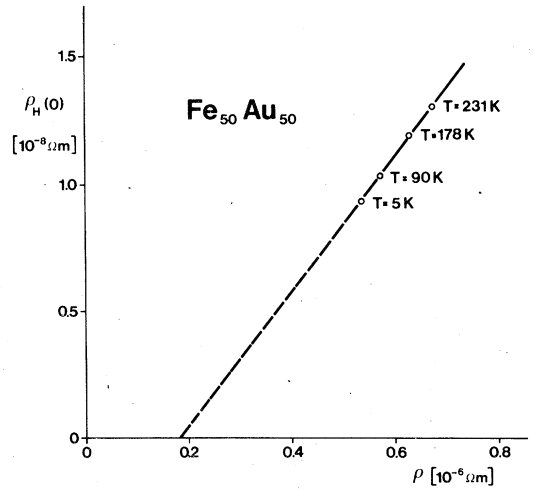

FIG. 10. Spontaneous Hall resistivity $\rho_H(0)$ of amorphous $Fe_{0.50}Au_{0.50}$ as a function of the resistivity ρ. The temperature T is the parameter.

havior is somewhat strking at first glance. We shall come back to this point in the discussion.

III. DISCUSSION

A. Isotropic resistivity

The theoretical description of the transport phenomena and of the resistance anisotropy in amorphous ferromagnets constitutes a very complicated problem. The basic idea for calculating the resistivity of a simple liquid or amorphous metal is due to Ziman.[17] Ziman considers the conduction electrons as free electrons which are independently scattered by each atom. The scattered waves interfere corresponding to the structure factor $a(q)$ of the metal. This leads to the well-known Ziman formula for the resistivity:

$$\rho = \frac{12\pi\Omega_0}{\hbar e^2 v_F^2} \int_0^1 d\left(\frac{q}{2k_F}\right)\left(\frac{q}{2k_F}\right)^3 a(q)|V_q|^2 , \quad (3.1)$$

where Ω_0 is the atomic volume, $a(q)$ is the structure factor, V_q is the pseudopotential, $k_F = (3\pi^2 z_{te}/\Omega_0)^{1/3}$ the Fermi wave vector with z_{te} number of free electrons per atom, and v_F^2 is the Fermi velocity. This formula has been extended to alloys by Faber and Ziman.[10]

One of the decisive suppositions of the Ziman and the Ziman-Faber theory is the assumption that the atoms in the amorphous or liquid metal (alloy) act as independent scatterers. Therefore the formula mainly involves the scattering properties of a single atom when dissolved in a matrix of identical atoms. Making use of this fact, Evans *et al.*[20] extended Ziman's formula to liquid and amorphous transition metals (TM). As the scattering by TM is considerably stronger and can be treated as resonance scattering, the Born approximation is no longer adequate for the description of an individual scattering process. Instead, the scattering by a single atom is exactly described by a t matrix $t(q)$. The generalized Ziman–Faber formula for TM is obtained by replacing V_q by t_q. This formula is known as the single-site approximation. After Friedel[30,31] the t matrix can be expressed in terms of phase shifts δ_l.

$$t(q) = \frac{2\pi\hbar^2}{m k_F \Omega_0} f_q ,$$

$$f_{kk'} = f_{k-k'} \quad (3.2)$$

$$= \sum_l (2l+1) P_l(\hat{k}\hat{k}') e^{i\delta_l} \sin\delta_l ,$$

where Y_{lm} are special harmonics; P_l are the Legendre polynominals of order l, k, k' unit vectors and their dot product $\hat{k}\cdot\hat{k}' = \cos\theta$.

The single-site approximation has been used in a number of papers[32–37] to calculate the resistivity of liquid and amorphous transition metals and ferromagnets. Its application to amorphous ferromagnets is quite problematic. In an amorphous ferromagnet the d states of spin-up and spin-down electrons are shifted with respect to each other because of the repulsive exchange interaction between opposite spins. The different occupations of the spin-up and spin-down states lead to different phase shifts $\delta_2^{\uparrow}$ and $\delta_2^{\downarrow}$ and consequently to different resistivities $\rho^{\uparrow}$ and $\rho^{\downarrow}$. This effect manifests itself particularly in the different resistivities in the ferromagnetic and paramagnetic states.[12]

In the case of amorphous ferromagnets a simple generalization of the Ziman-Evans formula offers

$$\rho^{\uparrow\downarrow} = \frac{24\pi\Omega_0}{e^2\hbar v_F^2} \int_0^1 d\left(\frac{q}{2k_F}\right)\left(\frac{q}{2k_F}\right)^3 a(q)|t_{kk'}^{\uparrow\downarrow}|^2 , \quad (3.1')$$

$$t_{kk'}^{\uparrow\downarrow} = \frac{2\pi\hbar^2}{m k_F \Omega_0} \sum_l (2l+1) e^{i\delta_l^{\uparrow\downarrow}} \sin(\delta_l^{\uparrow\downarrow}) P_l(\hat{k}\cdot\hat{k}') .$$

The spin-orbit interaction which will mix the $d^{\uparrow}$ and $d^{\downarrow}$ states has been neglected in this formula. For magnetic amorphous Fe, however, no d-phase shifts δ_2 are available. For nonmagnetic amorphous Fe Waseda and Wright[34] obtained $\delta_0 \approx -0.4$, $\delta_1 = -0.04$, $\delta_2 = 2.8$. For the amorphous state of the neighboring elements Mn and Co, they obtained $\delta_2 = 2.65$ (Mn) and $\delta_2 = 2.9$ (Co). Almost identical values were calculated by Hirata *et al.*[33] for the corresponding liquid metals. The calculation of the resistivity allows some arbitrariness. First, the number of conduction electrons is generally set $z = 1$. Since z determines $2k_F$ and therefore the cutoff of the structure factor in the integral, the value of ρ depends rather sensitively on z. In addition, the structure factor of amorphous Fe, which is not stable in thick films, is not known sufficiently well. Waseda and Wright take this as one possible reason that their theoretical values for ρ are to small. Meisel and Cote[35] used the Percus–Yevick[38] hard-sphere model to calculate the factors of NiP.

We want to demonstrate how sensitively the calculated value of ρ depends on the different parameters. In Fig. 11(a) the resistivity is plotted as a function of the number z of conduction electrons per atom. The phase shifts are taken for nonmagnetic Fe ($\delta_0 = -0.4$, $\delta_1 = -0.04$, $\delta_2 = 2.8$). Experimentally, the structure factor is not known very accurately. Therefore we calculate it by means of the Percus–Yevick equation[38] as given by Ashcroft and Lekner.[39] For liquid metals, a filling factor η of 0.45 is optimal. The filling factor, $\eta = 0.50$, yields 3.2 for the maximum value in the structure factor. This agrees quite well with

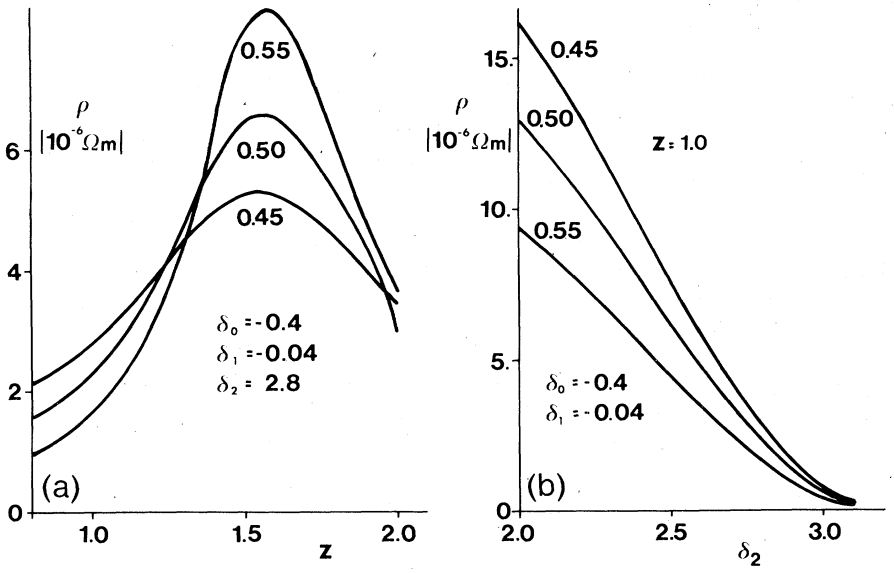

FIG. 11. (a) Resistivity as a function of the number of conduction electrons and (b) the resistivity as a function of the phase shift δ_2. The structure factor has been calculated by means of the Percus-Yevick equations. The numbers at the curves give the filling factors.

the experimental values in amorphous transition metals.[40] The use of the theoretical structure factors has the advantage that the choice of the valence z determines the relative position of $2k_F$ in the curve of the structure factor. Therefore a small inaccuracy in the atomic volume yields only a small error in the final value of the resistivity. For comparison, we also plot the result for $\eta = 0.55$. This filling factor has been used by Meisel and Cote[35] in their calculation. The maximum value of the structure factor for $\eta = 0.55$ is 4.2 and lies above the experimental values. In Fig. 11(b) the resistivity is plotted as a function of δ_2 taking $z = 1$ and δ_0 and δ_1 as before. Again the filling factor is the parameter. The curves demonstrate the large variation of ρ with z, δ_2 and the structure factor. Therefore it is quite easy to reproduce the experimental value of ρ by a suitable choice of parameters. We believe, however, that a reliable calculation is only possible when the parameters are known accurately enough. This is not yet the case. In particular an exact calculation of $\delta_2^\uparrow$ and $\delta_2^\downarrow$ is necessary.

The phase-shift treatment qualitatively accounts for the concentration dependence of ρ (cf. Fig. 9) and especially for the increasing resistivity between 90- and 100-at.% Fe. For the Fe_cAu_{1-c} alloys the magnetic moment μ per Fe atom is about $3\mu_B$ for $0.45 < c < 0.9$ and drops towards $2\mu_B$ above 90-at.% Fe (cf. Fig. 6). We interpret this drop of μ as originating in a transfer of spin-up d electrons into spin-down d states. The phase shifts $\delta_2^\uparrow$ and $\delta_2^\downarrow$ approach each other. The difference between $\rho^\uparrow$ and $\rho^\downarrow$ is reduced and ρ increases. This interpretation is supported by a comparison with liquid alloys. We shall turn back to the point in Sec. III F.

B. Resistivity anisotropy

1. Anomalous Hall effect

A great number of theoretical works dealt with the anomalous Hall effect in crystalline ferromagnetic metals.[41-44] For further references see Refs. 45–47. In these works somewhat different (and sometimes even opposite) mechanisms are proposed. Smit[47] considered the d states as a superposition of spin-up and spin-down states due to the spin-orbit interaction. These mixed resonance states yield a scattering anisotropy. Berger[44] introduced the side-jump mechanism. Since all these theories require parameters which are badly known it is almost impossible to distinguish which mechanism is the dominant one. We want to discuss the resistance anisotropy within a model originally suggested by Fert and Jaoul[21] for the contribution of isolated magnetic atoms to the anomalous Hall effect. They started with the Friedel-Anderson model[30,48] for a magnetic atom and additionally introduced the spin-orbit coupling $\lambda \vec{s} \cdot \vec{l}$ which splits the fivefold-degenerate spin-up and spin-down resonance states as shown in Fig. 12. Now the resonance energy ϵ_{dm} also depends on the magnetic quantum number m:

$$\epsilon_{dm}^{\uparrow\downarrow} = \epsilon_{d0}^{\uparrow\downarrow} + \lambda s_z m , \tag{3.3}$$

which leads to phase shifts δ_{lm} which also depend on m.

We find for the scattering amplitude for the transition from k to k'

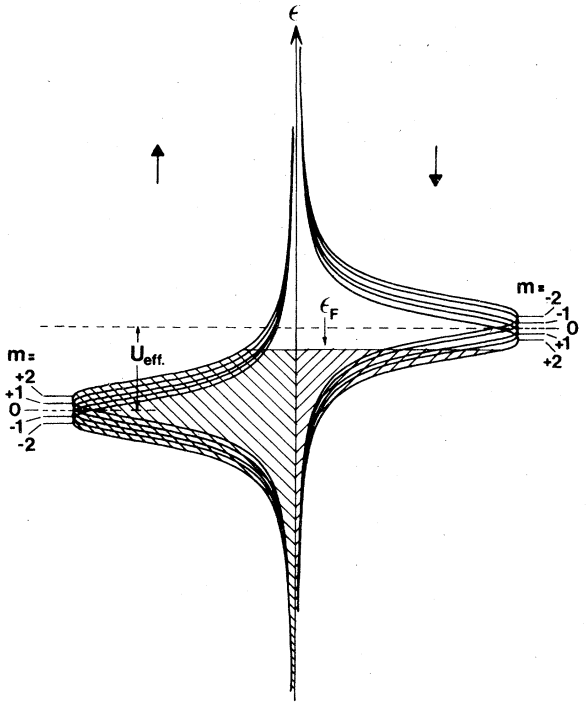

FIG. 12. Splitting of the resonance states of a magnetic atom due to exchange interaction and spin-orbit coupling [see Fert and Jaoul (Ref. 21)]. The variable on the horizontal axis is the density of states.

$$f_{kk'}^{\uparrow\downarrow} = 4\pi \sum_{l,m} Y_{lm}^*(\hat{k}) Y_{lm}(\hat{k}') e^{i\delta_l^{\uparrow\downarrow}} \sin\delta_l^{m\uparrow\downarrow}. \tag{3.4}$$

In this form, the scattering amplitude not only includes the difference between the momentum k and k' but also k and k' separately which gives rise to anisotropic scattering.

We prefer this model for the asymmetric scattering because it yields qualitatively the change in sign of the anomalous Hall effect in the series going from amorphous Fe to Co to Ni alloys.[9] In principle, it can be incorporated into the single-site approximation. However, the same difficulties as in the calculation of the isotropic resistivity arise also here. Therefore we restrict ourselves to the case of a dilute ferromagnet with low Fe concentration c. In analogy to the calculation of Fert and Jaoul one obtains for the cross section of the Hall resistivity

$$\sigma_H^{\uparrow\downarrow} = \frac{24\pi}{k_F^2} \sin\delta_1 \sin(2\delta_2^{\uparrow\downarrow} - \delta_1) \sin^2\delta_2^{\uparrow\downarrow} \frac{s_z\lambda}{\Gamma}$$

and (3.5)

$$\rho_H^{\uparrow\downarrow} = (m v_F c / z^{\uparrow\downarrow} e^2) \sigma_H .$$

For small Fe concentrations the magnetic moment of the Fe atoms is about $3\mu_B$. Here the Friedel sum rule[30] should work quite well. We take $\delta_1 = -0.04$ as before, $\delta_2^{\uparrow} = \pi$ and $\delta_2^{\downarrow} = \frac{2}{5}\pi$, $z^{\uparrow\downarrow} = 0.5$ and $\Omega_0 = 17.0 \times 10^{-30}\,\mathrm{m}^3$ (for Au). For the relative splitting of the resonance curves due to spin-orbit coupling we choose $\lambda/\Gamma = 0.2$. These values yield for the Hall cross sections, $\sigma_H^{\downarrow} = 1.0 \times 10^{-21}\ \mathrm{m}^2$ and $\sigma_H^{\uparrow} = 0$. The Hall resistivity of the spin-down electrons is $\rho_H^{\downarrow} = 1.0 \times 10^{-7} c\ \Omega\,\mathrm{m}$. Because of the shunt of spin-up electrons, the Hall resistivity is reduced according to the relation

$$\rho_H = \rho_H^{\uparrow}(\rho^2/\rho^{\uparrow 2}) + \rho_H^{\downarrow}(\rho^2/\rho^{\downarrow 2}) . \tag{3.6}$$

For small Fe concentrations this gives $\rho_H \approx 2.5 \times 10^{-8} c\ \Omega\,\mathrm{m}$. The observed Hall resistivity is of this order of magnitude.

The strong increase of $\rho_H(0)$ towards pure Fe can be explained in the same model used before for the qualitative discussion of ρ. For $c > 90$-at.% Fe, $d^{\uparrow}$ electrons are transferred into $d^{\downarrow}$ states. For two reasons, this leads to an enhancement of ρ_H: (i) the spin-up electrons also undergo resonant scattering and this reduced their short-circuit effect, and (ii) their effective contribution to the Hall effect adds to that of the spin-down electrons, which is easily seen from Eq. (3.5). The occupation of spin-up resonance levels still corresponds to a phase shift $\delta_2^{0\uparrow}$ which is considerably greater than $\frac{1}{2}\pi$, changing the sign of the sine term in (3.5). At the same time, the term sequence of the magnetic quantum number m ($-2 \le m \le 2$) is reversed because now s_z is positive. Both changes in sign together yield an additive contribution to the Hall resistivity.[21]

The rapid increase of the anomalous Hall effect as one approaches the pure amorphous Fe is a characteristic feature of Fe. In the corresponding concentration range the anomalous Hall effect in amorphous $Co_c Au_{1-c}$ and $Ni_c Au_{1-c}$ alloy varies only weakly with c and passes through a maximum below $c = 1$.[9,49] The different behavior of the $Fe_c Au_{1-c}$ system is correlated to the decrease of μ in this concentration range.

The Hall effect in the amorphous metallic glass $Fe_{0.80}P_{0.13}C_{0.07}$ has been measured and agrees surprisingly well with the result in pure Fe.[50] The anomalous Hall effect in pure Fe yields a Hall angle of 5°.

2. *Diagonal resistivity anisotropy*

The difference between $\rho_\parallel$ and $\rho_\perp$ can be calculated under the same assumption as the anomalous Hall effect. We restrict ourselves again to small Fe concentrations. Assuming dominating d scattering we calculate the difference in cross section $\Delta\sigma = \sigma_\parallel - \sigma_\perp$ to

$$\Delta\sigma^{\uparrow\downarrow} = \frac{24\pi}{k_F^2} \sin^4\delta_2^{\uparrow\downarrow}(1 - 4\cos^2\delta_2^{\uparrow\downarrow})\left(\frac{\lambda s_z}{\Gamma}\right)^2 ,$$
$$\Delta\rho^{\uparrow\downarrow} = \frac{m v_F c}{z^{\uparrow\downarrow} e^2} \Delta\sigma^{\uparrow\downarrow} . \tag{3.7}$$

Using the same values for the parameters as before in the calculation of the anomalous Hall effect we obtain $\Delta\sigma^{\downarrow} = 2.6\times10^{-21}$ m^2 and $\Delta\sigma^{\uparrow} = 0$. The resistance anisotropy is correspondingly $\Delta\rho^{\downarrow} = 2.6\times10^{-7} c\ \Omega$ m. Like the Hall effect, this anisotropy is reduced in the same manner by the shunt of the spin-up electrons. For small Fe concentrations, this yields a reduction by a factor of 4. The theoretical prediction is somewhat larger than the experimental values. This is not a serious problem because the splitting of the resonance curves is only estimated.

Surprisingly, $\rho_\parallel - \rho_\perp$ shows practically no dependence on the alloy composition (see Fig. 8). This is most striking in the high-concentration range $c > 0.9$ where the anomalous Hall effect increases drastically. The different behavior of $\rho_H(0)$ and $\rho_\parallel - \rho_\perp$ however, is understood by means of Eq. (3.7). Only for $1.05 \leq \delta_2^{0\uparrow\downarrow} \leq 2.09$, that is for $1.67 \leq z_d^{\uparrow\downarrow} \leq 3.3$ do we find $\rho_\parallel > \rho_\perp$. Therefore the spin-up electrons tend to compensate the resistivity anisotropy above 90-at.% Fe and qualitatively make comprehensive the weak dependence of $\rho_\parallel - \rho_\perp$ on the concentration.

We sketch the heuristic physical reason for the anisotropic scattering. Let a plane wave $\vec{k} = (k_x, 0, 0)$ with spin down be scattered by a ferromagnetically aligned atom (see Fig. 11). The plane wave then makes virtual transitions into the d-resonance states belonging to different values of m. Being proportional to the density of d states, the transition probability into the $m<0$ states is larger than that into the $m>0$ states. Roughly speaking the conduction electron is more likely to surround the scattering atom in the direction corresponding to $m<0$ than in the other direction.[51] This heuristic consideration in reality only holds if one takes into account the interference with p (or f) scattering. This interference leads to the left-right asymmetry known as the anomalous Hall effect.

A similar explanation holds for the anisotropy $\sigma_{zz} - \sigma_{xx}$. Due to the cylindrical symmetry of the problem, an electron wave entering from the z direction will experience scattering only into the $m=0$ state whereas coming from the x direction it will also scatter into the $m\neq0$ states. In both cases, the scattering probabilities will differ from each other.

From this heuristic interpretation as well as from the simplified relation (3.5) it is easily concluded that the anomalous Hall effect changes sign when the Fermi level passes the maximum of the resonance. Starting from a somewhat simple model for Fe, Co, and Ni atoms which assumes completely occupied spin-up states and spin-down states with two, three, and four d electrons, respectively, we see that between Fe and Ni, the Fermi level crosses the resonance maximum. Experimentally, we indeed observe a change of sign of the anomalous Hall effect which, however, takes place between Co and Ni. This might be due to the approximation used in (5) where mainly d scattering is taken into account.

Up to now, we assumed that the $d\uparrow$ and $d\downarrow$ states, respectively, are degenerate—except for the spin-orbit coupling. In the crystalline state, this degeneracy is generally split into T_{2g} and E_g states by crystal fields (in the case of an amorphous metal it is more adequate to call them "structure fields") and even more so by the boundary conditions of the wave functions in the Wigner-Seitz cell. A quantitative description of this splitting in an amorphous ferromagnet is very difficult. In Fig. 13 we compare a crystalline transition metal with an amorphous one (in two dimensions). Whereas the crystalline state exhibits an optimal overlap of the lobes and lowering of the band energy of these states, this overlap is not achieved on a significant scale in the amorphous state. Often the lobes reach into empty space.

From this, we draw the following conclusions

(i) The overlap $\langle d_1|V|d_2\rangle$ is reduced and so is the direct hopping probability for d electrons between neighboring atoms. This means a decrease of the mobility of the d electrons.

(ii) The forming of the lobes is reduced since they are no more suitable for an optimal overlap which means that the total density of the wave functions becomes more spherical.

(iii) Because of the reduced overlap we expect a smaller exchange integral and consequently a diminished Curie temperature.

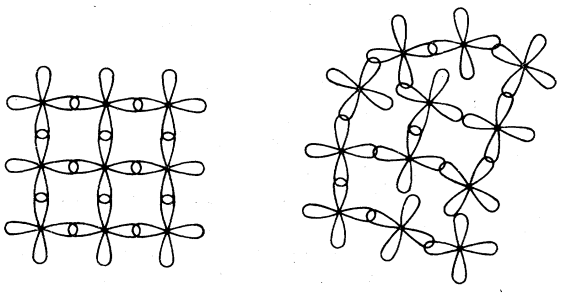

FIG. 13. Two-dimensional model for crystalline and amorphous transition metals demonstrating the reduced d-d overlap in the amorphous state.

(iiii) The reduced d overlap gives rise to a smaller ratio $\langle d_1|V|d_2\rangle:U$ of the transition-matrix element and the intra-atomic Coulomb energy U. On the large scale between band magnetism and localized magnetism, the reduced ratio $\langle d_1|V|d_2\rangle:U$ favors a shift towards the localized model.

C. Magnetoresistance $\partial\rho/\partial B$

Recently, one of the authors investigated the magnetoresistance in amorphous Ni_cAu_{1-c} alloys.[10] Up to now, the magnetoresistance in any amorphous ferromagnetic alloy of Fe, Co, and Ni with Au was found to be large and negative. Owing to the short mean-free path of the conduction electrons, the Lorentz force does not yield any measurable magneto-resistance effect. In[10] the following models have been discussed with regard to the magnetoresistance: (a) the band-magnetism model where the spin-up and spin-down Fermi levels are shifted relatively to each other by an applied magnetic field, (b) the Heisenberg model under the assumption of local easy axis, and (c) the resonance-scattering picture. Each of the three models yielded values far too small compared to the experimental magnetoresistance. The same statement holds for the results in the Fe_cAu_{1-c} system presented here. Especially the resonance-scattering model seems to fail. On one hand, $\partial\rho/\partial B$ should be of the order of $\mu_B/\Gamma \approx 5.8\times10^{-5}$ m^2/V sec ($\Gamma\approx 1$ eV) which is too small by a factor of 10. On the other hand, the magnetoresistance should increase monotonously between 90- and 100-at.% Fe because the Fermi level crosses both resonance curve sets. This is the supposition for magnetoresistance in the resonance picture. On the contrary, we find a pronounced maximum at about 90-at.% Fe which apparently is correlated to the sudden drop of the magnetic moment μ.

D. Normal Hall effect

In amorphous non-transition-metals the normal Hall effect is readily described with the free-electron model,[52,53] whereas in amorphous transition metals anomalous contributions have to be considered. In the case of amorphous ferromagnetic metals the anomalous part of the Hall effect can essentially be separated by saturating it. In the high-field region, however, some anomalous contribution may remain due to a high-field susceptibility and a field dependence of R_s. Both contributions can be estimated within the same models as the magnetoresistance in Sec. III C. In the framework of these theoretical considerations, the high-field contribution of the anomalous Hall effect should be negligible compared to the measured Hall effect. We cannot, however, content ourselves with this result because the same arguments would predict a much smaller magnetoresistance. As long as the latter effect is not understood in full, we must be careful about interpreting the high-field Hall effect as normal Hall effect.

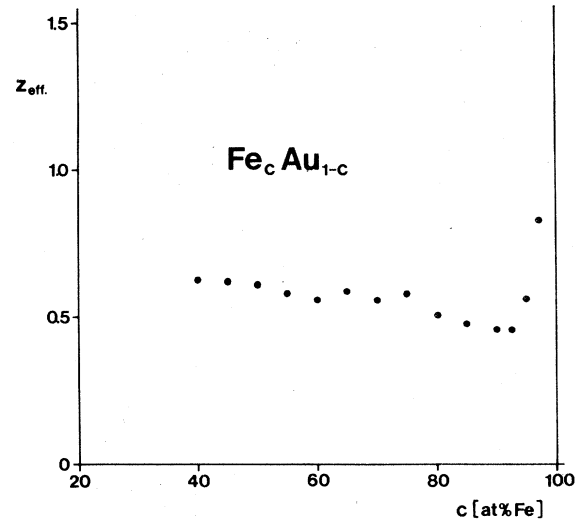

FIG. 14. Effective number of conduction electrons $z_{\rm eff}$ of the Fe_cAu_{1-c} alloys calculated from the high-field Hall constant R_∞.

Another difficulty typically met in ferromagnetic metals is that the mean-free paths of spin-up and spin-down electrons are not identical. So even if the free-electron model should be applicable the Hall constant always will yield an insufficient number $z_{\rm eff}$ of conduction electrons. For amorphous Ni_cAu_{1-c} alloys we recently found[8] that interpreting the high-field Hall effect as normal Hall effect yields reasonable results which agree with measurements above the Curie temperature.

From the high-field Hall constant R_∞ we calculate the effective numbers of conduction electrons $z_{\rm eff} = -\Omega_0/eR_\infty$. The result is shown in Fig. 14.

E. Thermal behavior of the spontaneous Hall resistivity

With the $Fe_{0.50}Au_{0.50}$ alloy we showed that the spontaneous Hall resistivity increases with T (Fig. 10). From the usual weakening of the magnetization one would rather expect a reduction of the effect at elevated temperatures. At the same time, the resistivity increases according to a T^2 law.[12] This increase of ρ arises from electron-magnon processes in which the conduction electron flips its spin. From the behavior of ρ_H we conclude that these spin-flip processes also exhibit a left-right asymmetry which compensates the thermal effect on ρ_H.

F. Comparison with liquid alloys

One of the reasons why we investigated the Fe_cAu_{1-c} alloys is that the liquid state of these systems has been extensively studied by Güntherodt and Künzi[16] and Güntherodt and Meier.[15] Among other features they found that the Hall effect becomes positive with increasing amount of Fe. In connection with our measurements, this positive Hall effect is easily understood. The liquid alloys are structurally equivalent to the amorphous ones. In all alloys investigated until present the Curie temperature in the disordered (amorphous or liquid) state lies below the melting point. Therefore the Fe atoms in the liquid are in a paramagnetic state and the suceptibility obeys a Curie-Weiss law. An externally applied field thus will polarize a nonvanishing part of the Fe atoms which then contribute to anisotropic scattering and especially to the anomalous Hall effect. Our data from the amorphous Fe_cAu_{1-c} alloys permit a qualitative comparison with results from liquid alloys. As an example, we choose $Fe_{0.50}Au_{0.50}$. The Hall constant extrapolated from measurements in the liquid state is $+13\times10^{-11}$ m^3 (A sec)$^{+1}$.[16] In the amorphous ferromagnetic state the spontaneous Hall resistivity is 0.95×10^{-8} Ω m. For the resistivity of liquid $Fe_{0.50}Au_{0.50}$ of $\rho_l = 1.73\times10^{-6}$ Ω m (which is taken from Fig. 9) the ρ_H curve in Fig. 10 would extrapolate to $\rho_H \approx 4\times10^{-8}$ Ω m. This rough estimate though corresponds to a rather artificial state combining the full ferromagnetism of the amorphous alloy with the spin-flip processes of the liquid.

Neglecting the influence of the structure factors in both amorphous and liquid state for simplicity, one should expect that the contribution to the anomalous Hall effect is proportional to the magnetization J_s. The constant of proportionality is given by $\rho_H(0)/J_s$. We denote the contribution of the anomalous Hall effect to the Hall constant with R_H^a and have $\rho_H(0)/J_s = R_H^a/\chi$. In liquid $Fe_{0.50}Au_{0.50}$ the susceptibility χ amounts to about 17.5×10^{-4} emu/g ("=" 2.4×10^{-3} mks units)[15] and $J_s \approx 1.4$ V sec m^{-2}. From these data we estimate a contribution of $R_H^a \approx 7\times10^{-11}$ m^3/A sec. This rough estimate yields a value which—though too small—tends to compensate the normal Hall effect and is of the right order of magnitude. With increasing Fe concentration, the anomalous contribution increases because both χ and $\rho_H(0)$ grow.

In Fig. 9 we compare the resistivity of the amorphous and the liquid phases (the dashed part of the ρ_{liquid} curve is extrapolated). The resistivity $\rho_{\text{amorphous}}$ is distinctly smaller than ρ_{liquid} which we attribute to the difference between the spin-up and spin-down partial resistivities. In the liquid state, one has, due to the spin disorder, no partial short circuiting by one spin polarization[54] (see Sec. III A). This interpretation is supported by the behavior near pure Fe and pure Au. In pure amorphous Au (which, however, is not stable) $\rho^\uparrow$ and $\rho^\downarrow$ should be identical and $\rho_{\text{liquid}} \approx \rho_{\text{amorphous}}$, which fits fairly to the extrapolated curve. In pure Fe the differences between $\rho^\uparrow$ and $\rho^\downarrow$ diminishes, too, because both spin directions of the conduction electrons are scattered resonantly. Therefore, the difference between ρ_{liquid} and $\rho_{\text{amorphous}}$ is smaller. This is confirmed by the experiment.

IV. CONCLUSION

We have investigated the electrical transport properties of amorphous ferromagnetic Fe_cAu_{1-c} alloys. The resistivity is anisotropic with respect to the direction of magnetization. It shows an anomalous Hall effect and different values parallel and perpendicular to the magnetization. All components are field dependent. Most properties depend on the Fe concentration in a characteristic manner at 90% Fe. This is correlated with the sudden drop of the magnetic moment above 90% Fe. The theoretical model for the calculation of the residual resistivity, in amorphous ferromagnets is discussed. We suggest that the single-site approximation originally derived for liquid transition metals should be modified for amorphous ferromagnets. The phase shift δ_2 should be replaced by two different phase shifts $\delta_2^\uparrow$ and $\delta_2^\downarrow$ for spin-up and spin-down scattering. A numerical calculation of these phase shifts would be quite valuable for a better discussion of the resistivity. The different resistivities in the ferromagnetic and the paramagnetic state and in the liquid state support this idea. The resistance anisotropy is discussed semiquantitatively for small Fe concentrations in a resonance picture. The anomalous Hall effect in the ferromagnetic amorphous state also yields a qualitative understanding of the positive Hall effect in the liquid Fe_cAu_{1-c} system.

We regard these investigations in connection with the transport properties of ferromagnetic glasses. Compared to the latter, the properties of the amorphous Fe_cAu_{1-c} system (among others) are surveyed more easily. Here, the number of conduction electrons, the number of different scattering potentials, and the range of the relevant structure factors allow a better quantitative comparison between theory and experiment. We think that a satisfying agreement between experi-

mental results and theoretical models must be sought first for these simple systems before the theoretical description of metallic glasses will prove to be successful.

ACKNOWLEDGMENT

The experiments have been generously sponsored by the Deutsche Forschungsgemeinschaft.

---

[1]Some amorphous metals like $Au_x La_{100-x}$ with high crystallization temperatures can also be obtained by splat cooling [W. L. Johnson, S. J. Poon, and P. Duwez, Phys. Rev. B 11, 150 (1975)].

[2]K. Handrich, *Magnetische Eigenschaften von Festkörpern* (VEB Deutscher Verlag für Grundstoffindustrie, Leipzig, 1975), p. 169.

[3]G. S. Cargill, III, in Proceedings of the International Conference on Electronic and Magnetic Properties of Liquid Metals, Mexico, 1975 (unpublished).

[4]H. S. Chen, Mater. Sci. Eng. 25, 59 (1976).

[5]R. Hasegawa, R. C. O'Hendley, and L. I. Mendelson, AIP Conf. Proc. 34, 298 (1976).

[6]T. Egami, J. Am. Ceram. Soc. (to be published).

[7]F. E. Luborsky, *Amorphous Magnetism II,* edited by R. A. Levy and R. Hasegawa (Plenum, New York, 1977).

[8]G. Bergmann, Solid State Commun. 18, 897 (1976).

[9]G. Bergmann, Z. Phys. B 25, 255 (1976).

[10]G. Bergmann, Phys. Rev. B 15, 1514 (1977).

[11]G. Bergmann, Phys. Lett. A 60, 245 (1977).

[12]G. Bergmann and P. Marquadt, Phys. Rev. B 17, 1355 (1978).

[13]M. Kohler, Z. Phys. 124, 772 (1948); 125, 679 (1949).

[14]W. Felsch, Z. Angew. Phys. 29, 217 (1970).

[15]H.-J. Güntherodt and H. A. Meier, Phys. Kondens. Mater. 16, 25 (1973).

[16]H.-J. Güntherodt and H. U. Künzi, Phys. Kondens. Mater. 16, 117 (1973).

[17]J. M. Ziman, Philos. Mag. 6, 1013 (1961).

[18]C. C. Bradley, T. E. Faber, E. G. Wilson, and J. M. Ziman, Philos. Mag. 7, 865 (1962).

[19]T. E. Faber and J. M. Ziman, Philos. Mag. 11, 153 (1965).

[20]R. Evans, D. A. Greenwood, and P. Lloyd, Phys. Lett. A 35, 57 (1971).

[21]A. Fert and O. Jaoul, Phys. Rev. Lett. 28, 303 (1972).

[22]A. N. Nesmeyanov, *Vapor Pressure of the Chemical Elements* (Elsevier, Amsterdam, 1963).

[23]S. Tolansky, Nature (Lond.) 152, 722 (1943).

[24]G. Bergmann, Phys. Rev. B 7, 4850 (1973).

[25]A more precise alignment with the applied field direction is achieved by observing the potential difference between electrodes 3 and 4. In a perfect parallel orientation of the film plane with $\vec{B}$ this potential difference will vanish for any value of B.

[26]C. M. Hurd, *The Hall Effect in Metals and Alloys* (Plenum, New York, 1972).

[27]We use SI units with $B = \mu_0 H + J$.

[28]R. Koepke and G. Bergmann, Z. Phys. B 21, 185 (1975).

[29]G. Bergmann (unpublished).

[30]J. Friedel, Can. J. Phys. 34, 1190 (1956); Nuovo Cimento Suppl. 7, 287 (1958).

[31]B. A. Messiah, *Quantum Mechanics* (North-Holland, Amsterdam, 1974), Vol. I.

[32]O. Dreiach, R. Evans, H.-J. Güntherodt, and H.-U. Künzi, J. Phys. F 2, 709 (1972).

[33]K. Hirata, Y. Waseda, A. Jain, and R. Srivastava, J. Phys. F 7, 419 (1977).

[34]Y. Waseda and J. G. Wright, Phys. Status Solidi B 181, K37 (1977).

[35]L. V. Meisel and P. J. Cote, Phys. Rev. B 15, 2970 (1977).

[36]P. J. Cote and L. V. Meisel, Phys. Rev. Lett. 39, 102 (1977).

[37]B. Steffen, Phys. Rev. B 13, 3227 (1976).

[38]J. K. Percus and G. J. Yevick, Phys. Rev. 110, 1 (1958).

[39]N. W. Ashcroft and J. Lekner, Phys. Rev. 145, 83 (1966).

[40]J. G. Wright, in Proceedings of the Seventh International Colloquium on Magnetic Thin Films, Regensburg, 1975 (unpublished).

[41]J. Smit, Physica 16, 612 (1951).

[42]R. Karplus and J. M. Luttinger, Phys. Rev. 95, 1154 (1954).

[43]J. Kondo, Progr. Theor. Phys. 27, 772 (1962).

[44]L. Berger, Phys. Rev. B 2, 4559 (1970).

[45]Proceedings of the Meeting: L'effect Hall Extraordinaire, Saint Cergue, 1972, edited by G. Cohen, B. Giovannini, and D. Sorg (unpublished).

[46]P. Nozières and C. Lewiner, J. Phys. (Paris) 34, 901 (1973).

[47]C. M. Hurd, *The Hall Effect in Metals and Alloys* (Plenum, New York, 1972).

[48]P. W. Anderson, Phys. Rev. 124, 41 (1961).

[49]G. Bergmann (unpublished).

[50]S. C. H. Lin, J. Appl. Phys. 40, 2175 (1969).

[51]C. M. Hurd, Contemp. Phys. 16, 517 (1975).

[52]G. Bergmann, Phys. Rep. 27C, 161 (1976).

[53]Only the heavy elements Tl, Pb, and Bi deviate from the free-electron model.

[54]In addition, spin-flip processes contribute to the resistivity of the liquid.

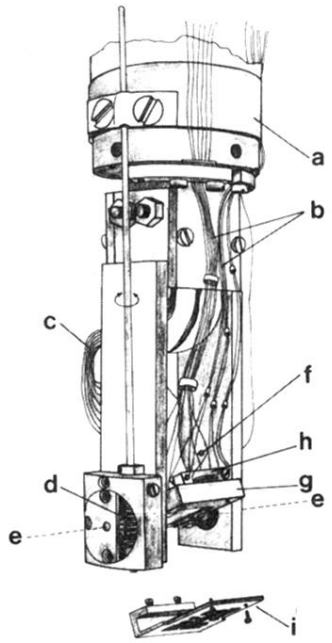

FIG. 2. Bottom part of our evaporation cryostat consisting of He tank (a) and rotatable sample holder (g) which is suspended by copper bars. The rotation about the axis *e-e* is performed by means of a worm and spur (d). Thermal coupling to (a) is achieved by flexible silver strips (c). The closing of an electrical circuit at (f) indicates the longitudinal orientation. The quartz substrate is mounted from below by means of the mask holder (i). Several thermometers are housed in part (h). The electrical leads are denoted by (b).